Metallomics

COMMUNICATION

View Article Online
View Journal

Cite this: DOI: 10.1039/c9mt00299e

Received 7th December 2019,
Accepted 18th February 2020

DOI: 10.1039/c9mt00299e

rsc.li/metallomics

Hierarchical binding of copper^{II} to N-truncated Aβ_{4-16} peptide†

Xiangyu Teng, ‡[a] Ewelina Stefaniak, ‡[b] Paul Girvan, [a] Radosław Kotuniak, [b] Dawid Płonka, [b] Wojciech Bal *[b] and Liming Ying *[c]

N-Truncated Aβ_{4-42} displays a high binding affinity with Cu^{II}. A mechanistic scheme of the interactions between Aβ_{4-42} and Cu^{II} has been proposed using a fluorescence approach. The timescales of different conversion steps were determined. This kinetic mechanism indicates the potential synaptic functions of Aβ_{4-42} during neurotransmission.

The amyloid-β (Aβ) peptides associated with Alzheimer's Disease (AD) comprise a number of species. The "canonical" Aβ_{1-42} and Aβ_{1-40} peptides derived directly by proteolysis of the Amyloid Precursor Protein (APP) are complemented by N- and C-truncated species, yielded by a variety of brain proteases.[1] Among them, the N-truncated Aβ_{4-42} has been reported as particularly abundant in the hippocampus and cortex of sporadic AD patients, as well as in healthy controls,[2,3] even exceeding Aβ_{1-42} and Aβ_{1-40}.[4,5] Aβ_{1-x} peptides can bind Cu^{II} using the N-terminus and H6, H13, and His14 residues.[6–8] Hence, Aβ_{1-16} has been adopted as a common model peptide in metal binding studies. K_d in the range of 0.1 nM to 1 nM at pH 7.1–7.4 was determined for Aβ_{1-16} and Aβ_{1-40}.[9–11] The adventitious binding of Cu^{II} ions to A$\beta_{1-42/40}$ and the concomitant generation of reactive oxygen species (ROS) *via* the Cu^{II}/Cu^{I} redox pair has been proposed to be the molecular basis of oxidative stress and neuronal death in AD.[12] On the other hand, Aβ_{4-x} peptides bind a Cu^{II} ion more than three orders of magnitude more strongly (K_d = 30 fM and 6.6 fM at pH 7.4 for Aβ_{4-16} and Aβ_{4-9}, respectively), using their N-terminal ATCUN motif spanning the Phe4, Arg5 and His6 residues. These complexes are redox-inert and do not generate significant ROS. Cu^{II} ion transfer from Aβ_{1-16} to Aβ_{4-16} occurs upon adding the latter to the Cu^{II}Aβ_{1-16} solution.[13]

Significance to metallomics

N-Truncated Aβ_{4-x} is abundant in both healthy and AD brains. Its Cu(II) binding affinity is three orders of magnitude stronger than well-known Aβ_{1-42} or Aβ_{1-40}. Using a model peptide, Aβ_{4-16}, we have elucidated the reaction mechanism of Cu(II) with Aβ_{4-x}, crucial to understand the physiological role and toxicity of Aβ peptides. The presence of two kinetic intermediates prior to the formation of the tight ATCUN complex has implications for the potential function of Aβ_{4-42} as a Cu(II) transporter during neurotransmission. The methodology used in this work may also stimulate the research of Cu(II) interactions with other intrinsically disordered proteins (IDPs).

This reaction is quantitative, in agreement with the affinity difference, and fast, occurring within the sample preparation time ~s. Such a reaction suggested that Aβ_{4-42} should prevail as a Cu^{II} binding Aβ species in the extracellular spaces of the brain. This finding gave rise to a hypothesis that Aβ_{4-42} may have a physiological role as a synaptic Cu^{II} scavenger during neurotransmission.[14] However, Cu^{II} release events in glutamatergic synapses may occur on a much faster, millisecond scale. Therefore, a thorough determination of association and dissociation rate constants for the participating species is necessary to help evaluate their relevance *in vivo*. Such data have been obtained previously for Cu^{II}Aβ_{1-x} complexes.[15–17] Here, we studied the reaction mechanism for Cu^{II} binding to the model peptide Aβ_{4-16} and found that the reaction follows a hierarchical fashion, going through two intermediate states and then reaching the final tight complex.

First, we studied the effect of N-truncation on the Cu^{II} binding kinetics. 20 nM Aβ labelled by HiLyte Fluor 488 on lysine 16 (FRHDSGYEVHHQK-HiLyte 488) was reacted with 400 nM Cu^{II} under various HEPES concentrations in order to obtain the HEPES-independent Cu^{II} binding rate constant (k_{on}). The results are shown in Fig. 1a. The intercept of the fitted curve (Fig. 1b) was used to determine k_{on}, which is 2.0(1) × 10^8 M^{-1} s^{-1}, 2.5 times slower than the value for Aβ_{1-16}.[17]

k_{off} was determined for the reaction of a Cu^{II} complex of unlabelled Aβ_{4-16} with an excess of EDTA. The estimated value

[a] Department of Chemistry, Imperial College London, Molecular Sciences Research Hub, White City Campus, London W12 0BZ, UK
[b] Institute of Biochemistry and Biophysics, Polish Academy of Sciences, Pawińskiego 5a, 02-106 Warsaw, Poland. E-mail: wbal@ibb.waw.pl
[c] National Heart and Lung Institute, Imperial College London, Molecular Sciences Research Hub, White City Campus, London W12 0BZ, UK. E-mail: l.ying@imperial.ac.uk

† Electronic supplementary information (ESI) available. See DOI: 10.1039/c9mt00299e
‡ These authors contributed equally to this work.

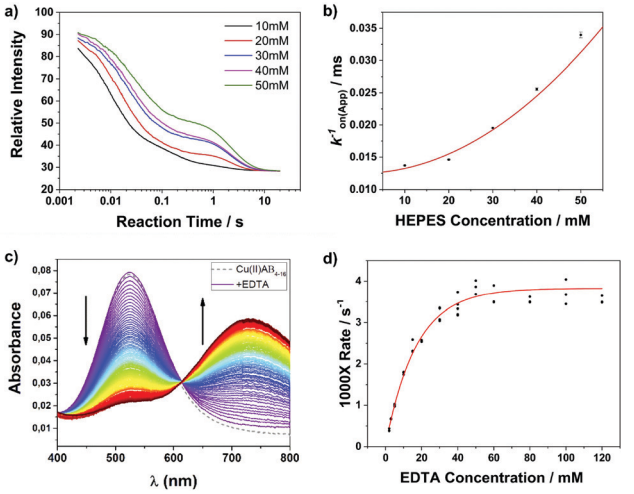

Fig. 1 Kinetics of Cu^{II} binding to $A\beta_{4-16}$. (a) Representative raw traces of Aβ (20 nM) with Cu^{II} (400 nM) under various concentrations of HEPES. The experiments were performed in 50 mM HEPES and 100 mM NaCl buffer solution at 298 K (pH 7.5). (b) HEPES dependence of k_{on}. The HEPES independent k_{on} value is 2.0(1) × 10^8 M^{-1} s^{-1}. (c) Kinetics of dissociation of $Cu^{II}A\beta_{4-16}$ assisted by varying concentrations of EDTA, monitored by UV-vis absorbance. The experiments were performed for 1 mM $Cu^{II}A\beta_{4-16}$ at 298 K (pH 7.5). (d) Empirical fit to derive the EDTA-independent k_{off}.

is ~5 × 10^{-5} s^{-1}, which divided by k_{on} proposed here gives K_d ~ 250 fM. EDTA is a stronger Cu^{II} chelator than $A\beta_{4-16}$, with a log β of 18.7, which can be recalculated into a conditional constant ^{C}K of 16.0 at pH 7.5.[18] This value is sufficiently higher than that of $Cu^{II}A\beta_{4-16}$, 13.53, to assure full Cu^{II} transfer, as demonstrated in Fig. 1c. The reaction was carried out for a range of EDTA/peptide ratios between 2 and 120. Pseudo-1st order kinetics for the Cu^{II} transfer reaction was observed for all experiments. The non-linear response of k_{off} to EDTA required the EDTA-independent k_{off} value to be determined by the extrapolation of the empirical exponential fit to these data, as shown in Fig. 1d.

To gain a glimpse of a possible reaction mechanism of Cu^{II} binding to N-truncated $A\beta_{4-16}$, we performed binding experiments at a 1:1 mixing ratio of Aβ to Cu^{II} with increasing concentration. In such experiments, the effect of the second Cu^{II} binding can be ignored, as the relevant log K is as low as 6.7.[13] The raw traces are shown in Fig. 2a. We noticed that the reaction process is becoming concentration independent after ~2 s (results from the fit are summarized in Table S1, ESI†). Thus we infer the existence of an intramolecular process following the initial Cu^{II} binding.

Next, a double mixing stopped flow technique was employed to further explore the potential intermediate complexes formed after the initial Cu^{II} binding. This technique was successfully applied to probe the interconversion between component I and component II Cu^{II} coordination species of $A\beta_{1-16}$ and $A\beta_{1-40}$.[17] 2 μM $A\beta_{4-16}$ and 2 μM Cu^{II} were mixed in a delay loop and after various delay times the reaction was "frozen" by adding an excess of EDTA (Fig. 2b). Taking advantage of the disparities in reactivity of different $Cu^{II}A\beta_{4-16}$ species with EDTA, the time evolution of the population of individual species could be

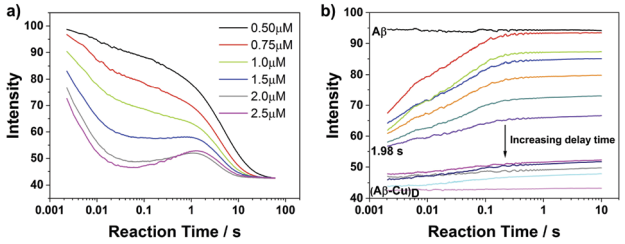

Fig. 2 (a) Raw traces of Cu^{II} binding measurements with a series of 1:1 concentration ratio HiLyte 488 labelled Aβ and Cu^{II} showing the evidence of intermediate species formation. The experiment was performed in 50 mM HEPES and 100 mM NaCl buffer solution at 298 K (pH 7.5). (b) Kinetics of HiLyte 488 labelled Aβ/Cu^{II} interactions measured by double mixing stopped flow. Raw traces showing the change in amplitude as the delay time between mixing of an equal concentration of Cu^{II} and Aβ (2 μM) and addition of EDTA is increased from 50 ms to 1 min. The experiment was performed in 50 mM HEPES and 100 mM NaCl buffer solution at 298 K (pH 7.5).

resolved and analyzed, enabling us to depict details of the binding process.

As shown in Fig. 2b, the amplitude of fluorescence recovery strongly depends on the delay time, indicating that a much more inert (less reactive towards EDTA) complex ("dark" complex) formed after around 2 s. We equate this end complex, $(A\beta–Cu)_D$, to the very stable ATCUN-type $Cu^{II}A\beta_{4-16}$ complex reported previously.[13] Furthermore, because the reaction rate is concentration independent after 2 s as mentioned above, we propose that a peptide conformational rearrangement process leading to this final complex must occur at around 2 s.

In order to describe the whole process of Cu^{II} binding of N-truncated $A\beta_{4-16}$, we hypothesized a reaction scheme as shown in Fig. 3a. The individual amplitudes of the two phases in Fig. 2b were determined by a global fit, which were further fitted by the scheme with KinTek software to validate it (Fig. 3b). The amplitudes indicate the amounts of two intermediates, Species I and Species II, at different reaction process stages, and could be

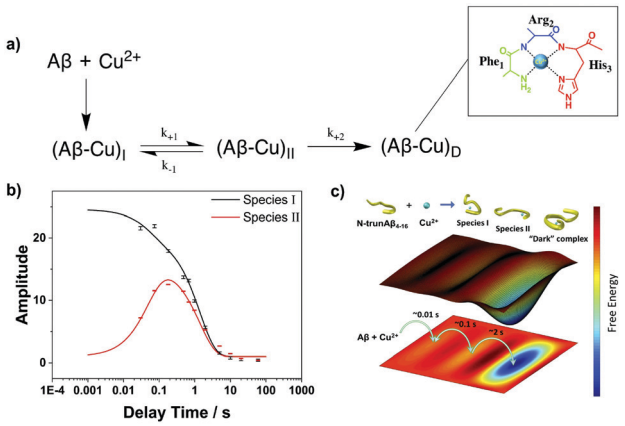

Fig. 3 (a) Reaction mechanism of Cu^{II} binding to $A\beta_{4-16}$ and formation of the high affinity $Cu^{II}A\beta_{4-16}$ complex, $(A\beta–Cu)_D$ (Cu^{II} binding site shown above). (b) Fitting of the individual amplitudes at different Cu^{II} binding process stages of the two phases by the predicted reaction mechanism. (c) Proposed free energy landscape of Cu^{II} binding to $A\beta_{4-16}$. "Dark" complex refers to the very stable ATCUN-type $Cu^{II}A\beta_{4-16}$ complex.

Table 1 Rate constants corresponding to the mechanism scheme shown in Fig. 3a

	k_{+1}	k_{-1}	k_{+2}
k value/s^{-1}	4.10(1)	10.34(2)	3.31(4)

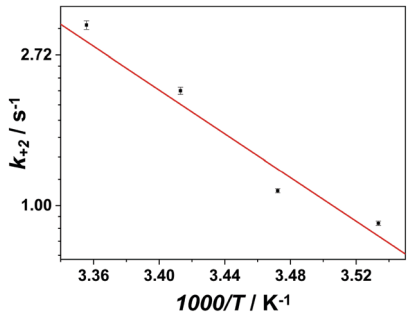

Fig. 4 Arrhenius plot for the switching rate constant k_{+2}. The switching activation energy determined is 64(3) kJ mol^{-1}.

fitted well by the predicted mechanism, with fitted rate constants listed in Table 1. A corresponding free energy landscape illustration of Cu^{II} binding with $A\beta_{4-16}$ is shown in Fig. 3c.

Finally, the activation energy of the $(A\beta\text{–}Cu)_D$ complex was determined to be 64(3) kJ mol^{-1} (Fig. 4) by performing a series of double mixing experiments at different temperatures (raw data shown in Fig. S1, ESI†).

The chemical properties of ATCUN Cu^{II} complexes of $A\beta_{4-x}$ peptides, such as high thermodynamic stability, absence of ROS production due to their resistance to oxidation and reduction, reluctance of copper to transfer to metallothionein-3 (MT3) and easy sequestering of Cu^{II} from $A\beta_{1-x}$, gave rise to a concept that $A\beta_{4-x}$ peptides (full-length $A\beta_{4-42}$ and its C-truncated analogs) may serve as guardians of synaptic function, by sequestering excess Cu^{II} ions released during neurotransmission in glutamatergic pathways.[14,19] The key unsolved issue is how these exchange-inert complexes relay copper back to neurons to maintain the proper copper cycling. Furthermore, Cu^{II}-free $A\beta_{4-42}$ can be neurotoxic by forming oligomeric species.[20] Detailed knowledge on mechanisms of Cu^{II} association with and dissociation from $A\beta_{4-x}$ peptides, represented here by $A\beta_{4-16}$, is thus crucial to understand the physiology and toxicity of these Aβ peptides.

The discovery of long-lived kinetic intermediates in the formation of the ATCUN complex of $A\beta_{4-16}$ is a game changer in the above considerations. The lifetimes of Species I and Species II complexes are comparable to the intervals between pulses of neurotransmitter release in glutamatergic neuronal pathways.[21] Therefore, these complexes may well contribute to the biological activity of $A\beta_{4-42}$, and of putative short peptidic fragments generated by neprilysin cleavage, such as $A\beta_{4-9}$.[22,23] There is only one way in which four nitrogen ligands of the ATCUN motif can be arranged around the Cu^{II} ion, and so it is reasonable to assume that the intermediate species contain the coordinatively unsaturated Cu^{II}. Such species have been implicated in the reverse reaction of Cu^{II} dissociative transfer from $Cu^{II}A\beta_{4-16}$ to MT3, to explain the catalytic effect of glutamate,[24] but it has not been observed directly. The Species I and in particular the longer-lived Species II complex may be the actual species able to move copper around during neurotransmission. The fact that the $Cu^{II}A\beta_{1-x}$ complex, although so much weaker, was formed 2.5 times faster, prompts further research into possible synaptic roles of Cu^{II} interactions with various Aβ species.

Furthermore, the observed hierarchical binding of Cu^{II} to $A\beta_{4-16}$ resembles the kinetics of the binding of many intrinsically disordered proteins (IDPs).[25] The methodology used in this study may be applicable to the fundamental understanding of the emerging "coupled binding and folding" paradigm.[26]

Conflicts of interest

There are no conflicts to declare.

Acknowledgements

This work was supported by the Leverhulme Trust grant RPG-2015-345 to LY and the Biotechnology and Biosciences Research Council (UK) grant BB/R022429/1 to LY, and the National Science Centre in Poland: PRELUDIUM Grant No. 2016/21/N/NZ1/02785 and ETIUDA Grant No. 2018/28/T/NZ1/00452, to ES, and OPUS Grant No. 2018/29/B/ST4/01634 to WB. The equipment used was sponsored in part by the Centre for Preclinical Research and Technology (CePT) under award number POIG.02.02.00-14-024/08-00, a project co-sponsored by European Regional Development Fund and Innovative Economy, the National Cohesion Strategy of Poland.

Notes and references

1 D. J. Selkoe, *Physiol. Rev.*, 2001, **81**, 741–766.
2 C. L. Masters, G. Simms, N. A. Weinman, G. Multhaup, B. L. McDonald and K. Beyreuther, *Proc. Natl. Acad. Sci. U. S. A.*, 1985, **82**, 4245–4249.
3 E. Portelius, N. Bogdanovic, M. K. Gustavsson, I. Volkmann, G. Brinkmalm, H. Zetterberg, B. Winblad and K. Blennow, *Acta Neuropathol.*, 2010, **120**, 185–193.
4 G. Antonios, N. Saiepour, Y. Bouter, B. C. Richard, A. Paetau, A. Verkkoniemi-Ahola, L. Lannfelt, M. Ingelsson, G. G. Kovacs, T. Pillot, O. Wirths and T. A. Bayer, *Acta Neuropathol. Commun.*, 2013, **1**, 56.
5 T. A. Bayer and O. Wirths, *Acta Neuropathol.*, 2014, **127**, 787–801.
6 P. Dorlet, S. Gambarelli, P. Faller and C. Hureau, *Angew. Chem.*, 2009, **121**, 9437–9440 (*Angew. Chem., Int. Ed.*, 2009, **48**, 9273–9276).
7 B. Alies, H. Eury, C. Bijani, L. Rechignat, P. Faller and C. Hureau, *Inorg. Chem.*, 2011, **50**, 11192–11201.
8 E. Atrián-Blasco, P. Gonzalez, A. Santoro, B. Alies, P. Faller and C. Hureau, *Coord. Chem. Rev.*, 2018, **375**, 38–55.
9 B. Alies, E. Renaglia, M. Rózga, W. Bal, P. Faller and C. Hureau, *Anal. Chem.*, 2013, **85**, 1501–1508.
10 T. R. Young, A. Kirchner, A. G. Wedd and Z. Xiao, *Metallomics*, 2014, **6**, 505–517.

11 A. Conte-Daban, V. Borghesani, S. Sayen, E. Guillon, Y. Journaux, G. Gontard, L. Lisnard and C. Hureau, *Anal. Chem.*, 2017, **89**, 2155–2162.
12 C. Cheignon, M. Jones, E. Atrián-Blasco, I. Kieffer, P. Faller, F. Collin and C. Hureau, *Chem. Sci.*, 2017, **8**, 5107–5118.
13 M. Mital, N. E. Wezynfeld, T. Frączyk, M. Z. Wiloch, U. E. Wawrzyniak, A. Bonna, C. Tumpach, K. J. Barnham, C. L. Haigh, W. Bal and S. C. Drew, *Angew. Chem.*, 2015, **127**, 10606–10610 (*Angew. Chem., Int. Ed.*, 2015, **54**, 10460–10464).
14 E. Stefaniak and W. Bal, *Inorg. Chem.*, 2019, **58**, 13561–13577.
15 P. Girvan, T. Miyake, X. Teng, T. Branch and L. Ying, *ChemBioChem*, 2016, **17**, 1732–1737.
16 T. Branch, M. Barahona, C. A. Dodson and L. Ying, *ACS Chem. Neurosci.*, 2017, **8**, 1970–1979.
17 T. Branch, P. Girvan, M. Barahona and L. Ying, *Angew. Chem.*, 2015, **127**, 1243–1246 (*Angew. Chem., Int. Ed.*, 2015, **54**, 1227–1230).
18 J. Felcman and J. J. da Silva, *Talanta*, 1983, **30**, 565–570.
19 N. E. Wezynfeld, E. Stefaniak, K. Stachucy, A. Drozd, D. Płonka, S. C. Drew, A. Krężel and W. Bal, *Angew. Chem.*, 2016, **128**, 8375–8378 (*Angew. Chem., Int. Ed.*, 2016, **55**, 8235–8238).
20 J. Dunys, A. Valverde and F. Checler, *J. Biol. Chem.*, 2018, **293**, 15419–15428.
21 W. Goch and W. Bal, *PLoS One*, 2017, **12**, e0170749.
22 M. Mital, W. Bal, T. Frączyk and S. C. Drew, *Inorg. Chem.*, 2018, **57**, 6193–6197.
23 K. Bossak-Ahmad, M. Mital, D. Płonka, S. C. Drew and W. Bal, *Inorg. Chem.*, 2019, **58**, 932–943.
24 A. Santoro, N. Wezynfeld, E. Stefaniak, A. Pomorski, D. Płonka, A. Krezel, W. Bal and P. Faller, *Chem. Commun.*, 2018, **54**, 12634–12637.
25 K. Sugase, H. J. Dyson and P. E. Wright, *Nature*, 2007, **447**, 1021–1025.
26 S. Gianni, J. Dogan and P. Jemth, *Curr. Opin. Struct. Biol.*, 2016, **36**, 18–24.